J. Fluid Mech. (1990), *vol.* 212, *pp.* 437–449
Printed in Great Britain

Stability of the laminar flow in a rectangular duct

By TOMOMASA TATSUMI[1] AND TAKAHIRO YOSHIMURA[2]

[1] Kyoto Institute of Technology, Kyoto 606, Japan

[2] Department of Physics, Faculty of Science, Kyoto University, Kyoto 606, Japan

(Received 17 July 1989 and in revised form 11 October 1989)

The stability of the laminar flow in a rectangular duct of an arbitrary aspect ratio is investigated numerically by expanding the flow fields of both the main flow and the disturbance into series of Legendre polynomials and solving the eigenvalue problem of the resulting matrix equation. The stability of the flow is found to depend upon the aspect ratio of the duct and the mode of the disturbance. The flow is unstable to two of the four possible modes of different parity and stable to the other two. With respect to the most unstable mode, the flow is stable or unstable according as the aspect ratio is below or above a critical value of 3.2 respectively, and the critical Reynolds number decreases monotonically with increasing aspect ratio towards the known value of 5772 for plane Poiseuille flow. The flow field of the disturbance shows the existence of strong vortex layers along the critical layer at which the velocity equals the phase velocity of the disturbance.

1. Introduction

It is well known that viscous flows with given boundaries are laminar at relatively small Reynolds numbers and become turbulent at large Reynolds numbers. The onset of turbulence in the flows is accounted for in terms of the instability of the corresponding laminar flows with respect to external disturbances. For flows of simple geometry, we can find certain critical values of the Reynolds number, under and above which the flows are stable and unstable respectively.

The notion of the stability of laminar flows is most clearly defined with respect to small disturbances, since the problem is then linearized with respect to the magnitude of disturbances and the stability characteristics of the flows become independent of the details of the disturbances. The linear theory of stability was first applied successfully by Tollmien (1929) and Schlichting (1933) to plane Poiseuille flow and the Blasius boundary layer and their theoretical results were first confirmed experimentally by Schubauer & Skramstad (1947). After the eminent achievements by these authors on the fundamental nature of fluid flows, the stability characteristics of laminar flows have been investigated in great detail both theoretically and experimentally, and developments in this field have brought about rapid progress in engineering applications.

The theory of stability has so far been applied to relatively simple laminar flows whose velocity distributions depend only upon a space variable at least in an approximate sense. Two-dimensional and axisymmetric flows including plane Poiseuille flow, the Blasius boundary layer, free mixing layers, jets and wakes belong to this category of flows. On the other hand, those flows that have more complex velocity distributions have been left untouched since the semi-analytical methods which were useful for the simple flows become cumbersome for the complex flows.

These flows may be treated more conveniently by numerical methods together with the orthogonal function expansion of the flow field. Thanks to recent progress in high-speed computation technology, such numerical analysis of the stability problem has now become available.

We investigate in this paper the stability of the laminar flow in a straight rectangular duct. This type of flow is often encountered in engineering practice, mostly in a turbulent state. While the current theoretical results on turbulent duct flows are mostly based on empirical closure assumptions, it seems desirable to clarify the fundamental mechanism of onset of these turbulent flows on a rigorous mathematical basis.

The stability of rectangular duct flows appears to deserve attention in itself. The aspect ratio, A say, of the rectangular cross-section varies from one to infinity. In the limit of $A = 1$, we have the flow in a square duct which seems to be stable in view of its similarity to the Hagen–Poiseuille flow in a circular tube whose stability had already been demonstrated (see Drazin & Reid 1981). In the other limit of $A \to \infty$, the duct flow tends to plane Poiseuille flow between two parallel planes which is known to be unstable with the critical Reynolds number $R_c = 5772$ (see Orszag 1971). Thus, there must exist some critical value of the aspect ratio, A_c say, below and above which the duct flow is stable and unstable respectively. It is interesting to work out quantitatively the stability characteristics of the duct flows, and in fact it will be shown below that $A_c = 3.2$ for the most unstable mode of the disturbance.

2. Mathematical formulation

The velocity $\boldsymbol{u}$ and the pressure p of the flow are governed by the following equations of motion and continuity:

$$\frac{\partial \boldsymbol{u}}{\partial t} + (\boldsymbol{u} \cdot \operatorname{grad}) \boldsymbol{u} = -\operatorname{grad} p + \frac{1}{R} \Delta \boldsymbol{u}, \tag{1}$$

$$\operatorname{div} \boldsymbol{u} = 0, \tag{2}$$

where all variables have been non-dimensionalized using a characteristic length L_0 and velocity U_0 of the flow, and

$$R = U_0 L_0 / \nu, \tag{3}$$

ν being the kinetic viscosity of the fluid, represents the Reynolds number characterizing the flow.

Take the rectangular coordinate $\boldsymbol{x} = (x, y, z)$ with the x-axis along the central axis of the duct and the y- and z-axes each parallel to the narrower and wider sidewalls respectively. If we express the widths of the narrower and wider walls as $2L_0$ and $2AL_0$ respectively, the walls are expressed in non-dimensional form as $y = \pm 1$, $z = \pm A$, where A ($\geqslant 1$) represents the aspect ratio of the rectangular cross-section of the duct. Then, the boundary conditions for (1) and (2) are given by

$$\boldsymbol{u} = 0 \quad \text{at} \quad y = \pm 1 \quad \text{and} \quad z = \pm A. \tag{4}$$

In order to solve the boundary-value problem related to (1), (2) and (4), we expand the velocity $\boldsymbol{u}$ and the pressure p into series of Legendre polynomials with respect to y and z, but the detailed expressions for the cases of the stationary laminar flow and its stability will be given separately.

3. Stationary laminar flow

If we assume the stationary laminar flow in a rectangular duct to be parallel to the axis of the duct and unchanged in the axial direction, the velocity $\boldsymbol{u}$ and the pressure p are expressed in the following form:

$$\left.\begin{aligned} \boldsymbol{u}(\boldsymbol{x},t) &= \boldsymbol{U}(\boldsymbol{x}) = (U(y,z),0,0), \\ p(\boldsymbol{x},t) &= P(\boldsymbol{x}). \end{aligned}\right\} \tag{5}$$

Substituting (5) into (1) and (2), we find that (2) is automatically satisfied and (1) is reduced to the following equations:

$$\frac{\partial P}{\partial x} = -\kappa = \text{const.}, \quad \frac{\partial P}{\partial y} = \frac{\partial P}{\partial z} = 0, \tag{6}$$

$$\left(\frac{\partial^2}{\partial y^2}+\frac{\partial^2}{\partial z^2}\right)U(y,z) = -R\kappa, \tag{7}$$

where κ is a positive constant representing the pressure drop downstream. It also follows from (4) that

$$U(y,z) = 0 \quad \text{at} \quad y = \pm 1 \quad \text{and} \quad z = \pm A, \tag{8}$$

which gives the boundary condition for (7).

The velocity distribution $U(y,z)$ of the stationary laminar flow is thus obtained by solving a two-dimensional potential equation (7) under the boundary condition (8). This problem has already been solved by Saint-Venant (1855) for the mathematically equivalent problem of the torsion of an elastic column with rectangular cross-section. He expressed the solution in terms of a series of trigonometric and hyperbolic functions and obtained mathematical expressions for the quantities corresponding to the velocity distribution $U(y,z)$ and the non-dimensional flux per unit time,

$$Q_{\text{nd}} = \int_{-1}^{1}\int_{-A}^{A} U(y,z)\,\mathrm{d}y\,\mathrm{d}z. \tag{9}$$

However, we shall employ expansions in terms of Legendre polynomials in view of the convenience of dealing with the stability problem in the same mathematical framework.

As easily seen from the linearity of the boundary-value problem, the magnitude of the solution $U(y,z)$ is proportional to $R\kappa$, so that if a solution is obtained for a certain value of $R\kappa$ the solution for an arbitrary value of $R\kappa$ is immediately derived from it. First, calculate a solution for $R\kappa = 2$ and find the value of $U(0,0)$ for $R\kappa = 2$. Then, putting

$$R\kappa = 2/(U(0,0) \quad \text{for} \quad R\kappa = 2), \tag{10}$$

we obtain the solution $U(y,z)$ which satisfies the condition,

$$U(0,0) = 1, \tag{11}$$

that is equivalent to adopting the dimensional velocity on the central axis of the duct as the characteristic velocity U_0.

Now, we expand the velocity $U(y,z)$ into a series of Legendre polynomials in the rectangular domain $-1 \leqslant y \leqslant 1$, $-A \leqslant z \leqslant A$. In view of the evenness of (7) and the

boundary condition (8) for both the variables y and z, the solution must be an even function of y and z and the expansion must involve only polynomials of even orders:

$$U(y,z)=\sum_{m=0}^{M}\sum_{n=0}^{N}U_{mn}P_{2m}(y)P_{2n}(z/A), \tag{12}$$

where P_m represents the Legendre polynomial of order m.

Equation (7) with $R\kappa=2$ is equivalent to the stationarity condition for the functional,

$$J[U]=\int_{-1}^{1}\int_{-A}^{A}\left[\left(\frac{\partial U}{\partial y}\right)^2+\left(\frac{\partial U}{\partial z}\right)^2-4U\right]\mathrm{d}y\,\mathrm{d}z. \tag{13}$$

Substituting (12) into (13) we obtain the following expression:

$$J[U]=\sum_{k,m=0}^{M}\sum_{l,n=0}^{N}U_{kl}(B_{klmn}U_{mn}-4C_{k0}C_{l0}), \tag{14}$$

with

$$\left.\begin{aligned}
B_{klmn}&=D_{km}C_{ln}+\frac{1}{A^2}C_{km}D_{ln},\\
C_{mn}&=\int_{-1}^{1}P_{2m}(x)P_{2n}(x)\,\mathrm{d}x=\frac{2}{4m+1}\delta_{mn},\\
D_{mn}&=\int_{-1}^{1}\frac{\mathrm{d}P_{2m}(x)}{\mathrm{d}x}\frac{\mathrm{d}P_{2n}(x)}{\mathrm{d}x}\mathrm{d}x\\
&=\begin{cases}2m(m+1) & \text{for}\quad m\leqslant n,\\ 2n(n+1) & \text{for}\quad m\geqslant n.\end{cases}
\end{aligned}\right\} \tag{15}$$

where δ_{mn} stands for Kronecker's delta. Applying the stationarity condition,

$$\partial U/\partial U_{kl}=0\quad\text{for}\quad k=0,1,\ldots,M;\quad l=0,1,\ldots,N, \tag{16}$$

to (14), we obtain the equations

$$\sum_{m=0}^{M}\sum_{n=0}^{N}B_{klmn}U_{mn}-2C_{k0}C_{l0}+2\alpha_l+2\beta_k=0, \tag{17}$$

for $$k=0,1,\ldots,M;\quad l=0,1,\ldots,N,$$

where the α_l and β_k represent indeterminate coefficients.

On substitution from (12), the boundary condition (8) is written in the form of the conditions for the U_{mn} as follows:

$$\sum_{m=0}^{M}U_{mn}=0\quad\text{for}\quad n=0,1,\ldots,N, \tag{18}$$

$$\sum_{n=0}^{N}U_{mn}=0\quad\text{for}\quad m=0,1,\ldots,M. \tag{19}$$

Equations (17), (18) and (19), being composed of $(M+1)(N+1)$, $(N+1)$ and $(M+1)$ equations respectively, constitute a closed system of linear equations for the same number of unknowns, the U_{mn}, α_l and β_k. By solving these equations numerically the coefficients U_{mn} are determined, and substituting the results into (12) yields the velocity distribution $U(y,z)$ for $R\kappa=2$. Then applying the transformation (10), we finally obtain the velocity distribution $U(y,z)$ which satisfies the condition (11).

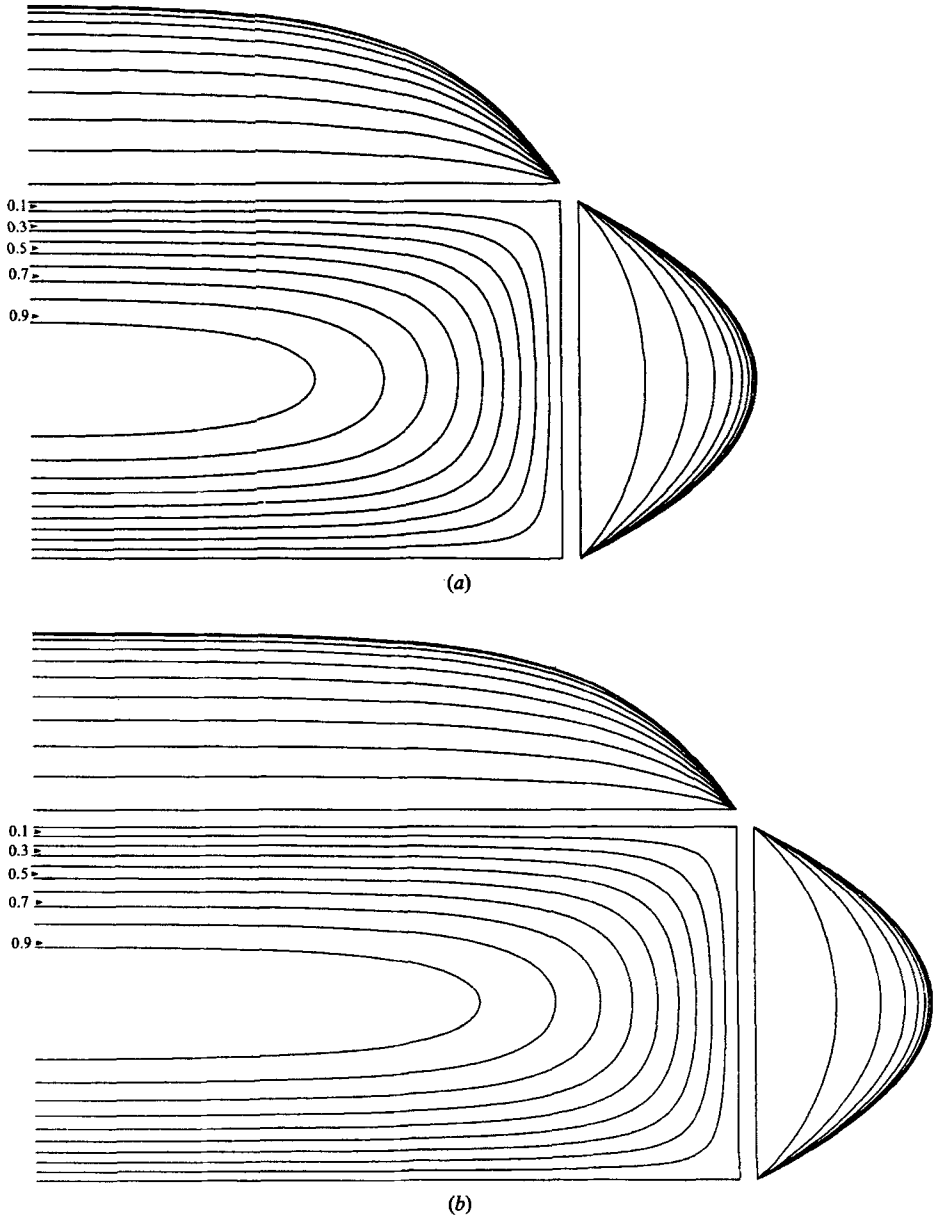

FIGURE 1. Isovelocity contours for $U = 0, 0.1, \ldots, 1.0$ and velocity profiles at sections, y or $z = 0, 0.1, \ldots, 1.0$. (*a*) $A = 3$, (*b*) $A = 4$.

4. Numerical results for the laminar flow

The numerical work has been carried out using FACOM VP200 and VP400 computers of the Data Processing Center of Kyoto University under the double-precision scheme.

The velocity distribution $U(y, z)$ has been calculated for the aspect ratios $A = 1, 2, \ldots, 5, 10, 20$ and 30. The number of terms in the expansion (12) have been chosen as $M = 20$ for all values of A, and $N = 20$ for $A \leqslant 3$, 30 for $A = 4$ and 5, and 40

A	1	2	3	4	5	10	20	30
$U(0, 0)$ for $R\kappa = 2$	0.58937	0.91097	0.98146	0.99615	0.99920	1.0000	1.0000	1.0000
$R\kappa$ for $U(0, 0) = 1$	3.3935	2.1955	2.0378	2.0077	2.0016	2.0000	2.0000	2.0000
$U_{00} = Q_{nd}/4A$ for $U(0, 0) = 1$	0.47704	0.50206	0.53658	0.56380	0.58310	0.62465	0.64566	0.65266
$Q_{nd}/4A$ for $R\kappa = 2$	0.28115	0.45736	0.52663	0.56163	0.58263	0.62465	0.64566	0.65266

TABLE 1. Non-dimensional fluxes Q_{nd} for constant maximum velocity ($U(0, 0) = 1$) and for constant pressure gradient ($R\kappa = 2$)

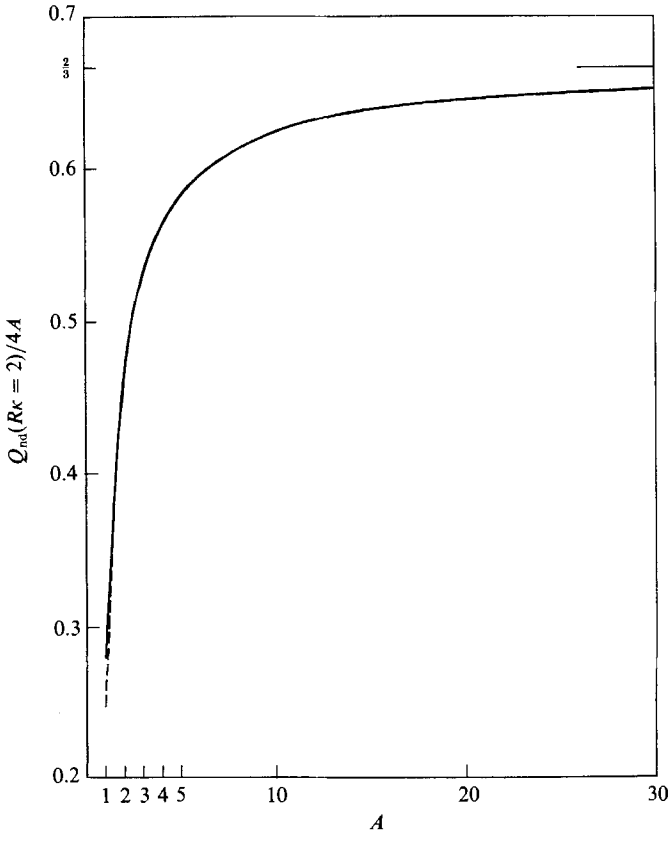

FIGURE 2. Non-dimensional flux $Q_{nd}(R\kappa = 2)$. The broken line refers to the formula (23).

for $A \geqslant 8$. These values of M and N have been confirmed to give accurate values to 10^{-6} digits for U_{mn}, $m \leqslant M$, $n \leqslant N$ and values less than 10^{-6} for U_{mn}, $m \geqslant M$, $n \geqslant N$.

The numerical results for $A = 3$ and 4 are shown graphically in figure 1 in the form of the isovelocity contours and the velocity profiles at various sections of constant y or z.

For large aspect ratios, $A \geqslant 5$ say, the velocity distribution in the central region

$4-A \leqslant z \leqslant A-4$ becomes almost identical to that of plane Poiseuille flow between two parallel planes,

$$U(y,z) = 1-y^2, \tag{20}$$

while it takes a universal distribution independent of A in the terminal regions $-A \leqslant z \leqslant 4-A$ and $A-4 \leqslant z \leqslant A$.

The non-dimensional flux Q_{nd} is easily derived from numerical result as

$$Q_{\mathrm{nd}} = 4AU_{00}, \tag{21}$$

which immediately follows from (12). The numerical result is given in table 1 and shown graphically in figure 2.

The dimensional flux Q_{d} under a given pressure gradient is immediately derived from Q_{nd} as

$$Q_{\mathrm{d}} = -\frac{1}{2\mu}\left(\frac{\mathrm{d}P}{\mathrm{d}x}\right)_{\mathrm{d}} L_0^4 Q_{\mathrm{nd}}(R\kappa = 2). \tag{22}$$

where $\mu = \rho\nu$ is the dynamic viscosity of the fluid.

Reflecting the asymptotic form of the velocity distribution $U(y,z)$ for large aspect ratios, Q_{nd} satisfies the following asymptotic formula for large A:

$$Q_{\mathrm{nd}}(R\kappa = 2)/4A = \tfrac{2}{3} - 0.4201/A, \tag{23}$$

where the constant has been determined by the numerical results for $A \geqslant 3$. Actually, (23) is valid for $A \geqslant 3$ within an error of 10^{-4}, so that it can be used as a practical formula for the flux of the flows for aspect ratios above 3.

5. Stability of the laminar flow

Now we proceed to the stability problem of the laminar flow in a rectangular duct which was obtained in the last section in the form of the Legendre polynomial expansion. Denoting the velocity and the pressure of a small disturbance by $\hat{\boldsymbol{u}}$ and $\hat{p}$ respectively, we can express the total velocity and pressure fields as follows:

$$\begin{pmatrix}\boldsymbol{u}\\ p\end{pmatrix}(\boldsymbol{x},t) = \begin{pmatrix}\boldsymbol{U}\\ P\end{pmatrix}(\boldsymbol{x}) + \begin{pmatrix}\hat{\boldsymbol{u}}\\ \hat{p}\end{pmatrix}(\boldsymbol{x},t). \tag{24}$$

If we decompose the disturbance fields into the Fourier series with respect to x, they may be written as

$$\begin{pmatrix}\hat{\boldsymbol{u}}\\ \hat{p}\end{pmatrix}(\boldsymbol{x},t) = \begin{pmatrix}\tilde{\boldsymbol{u}}\\ \tilde{p}\end{pmatrix}(y,z)\exp[\mathrm{i}\alpha(x-ct)], \tag{25}$$

where α represents the wavenumber along the x-axis and c is a complex constant generally dependent on α, $c = c_{\mathrm{r}} + \mathrm{i}c_{\mathrm{i}}$, c_{r} representing the phase velocity and αc_{i} the logarithmic amplification rate of the disturbance of the wavenumber α.

Substituting the decompositions (24) and (25) into (1) and (2) and taking into account that $\boldsymbol{U}$ and P of the laminar flow already satisfy the equations, we obtain a set of nonlinear equations for the disturbance amplitudes $\tilde{\boldsymbol{u}}$ and $\tilde{p}$. Since, however, we are dealing with small disturbances, we can neglect nonlinear terms with respect to $\tilde{\boldsymbol{u}}$ and $\tilde{p}$, and we obtain a set of linear equations for $\tilde{\boldsymbol{u}} = (\tilde{u},\tilde{v},\tilde{w})$ and $\tilde{p}$. Furthermore, eliminating $\tilde{u}$ and $\tilde{p}$ from these equations, we finally obtain the following simultaneous equations for the components $\tilde{v}$ and $\tilde{w}$:

$$\left.\begin{aligned}\mathscr{E}(y,z)\,\tilde{v} &= \mathscr{O}(y,z)\,\tilde{w},\\ \mathscr{E}(z,y)\,\tilde{w} &= \mathscr{O}(z,y)\,\tilde{v},\end{aligned}\right\} \tag{26}$$

where $\mathscr{E}$ and $\mathscr{O}$ are even and odd operators respectively defined as follows:

$$\mathscr{E}(y,z) = -\left[\frac{\mathrm{i}}{\alpha R}\left(\frac{\partial^2}{\partial y^2}+\frac{\partial^2}{\partial z^2}-\alpha^2\right)+(U-c)\right]\left(\frac{\partial^2}{\partial y^2}-\alpha^2\right)+\frac{\partial^2 U}{\partial y^2}, \tag{27}$$

$$\mathscr{O}(y,z) = \left[\frac{\mathrm{i}}{\alpha R}\left(\frac{\partial^2}{\partial y^2}+\frac{\partial^2}{\partial z^2}-\alpha^2\right)+(U-c)\right]\frac{\partial^2}{\partial y\,\partial z}-\frac{\partial U}{\partial z}\frac{\partial}{\partial y}+\frac{\partial U}{\partial y}\frac{\partial}{\partial z}-\frac{\partial^2 U}{\partial y\,\partial z}. \tag{28}$$

It is also understood that the exchange of y and z within the operators $\mathscr{E}$ and $\mathscr{O}$ in (26) does not apply to the arguments of $U(y,z)$ in (27) and (28). These equations give an extended version of the Orr–Sommerfeld equation for a basic flow of one-dimensional variation $U(y)$ (see Rosenhead 1963) to the case of two-dimensional variation $U(y,z)$.

The boundary conditions for (27) are immediately derived from (4) as follows:

$$\left.\begin{aligned}\tilde{v} = \tilde{w} = \partial\tilde{v}/\partial y = 0 \quad &\text{at} \quad y = \pm 1,\\ \tilde{v} = \tilde{w} = \partial\tilde{w}/\partial z = 0 \quad &\text{at} \quad z = \pm A.\end{aligned}\right\} \tag{29}$$

Since the Legendre polynomials themselves do not satisfy such boundary conditions, we construct the following combinations of the polynomials for the purpose of expressing $\tilde{v}$ and $\tilde{w}$:

$$\left.\begin{aligned}F_{2n} &= P_{2n+2}-P_0,\\ F_{2n+1} &= P_{2n+3}-P_1;\\ G_{2n} &= P_{2n+4}-\tfrac{1}{3}(n+2)(2n+5)P_2+\tfrac{1}{3}(n+1)(2n+7)P_0,\\ G_{2n+1} &= P_{2n+5}-\tfrac{1}{5}(n+2)(2n+7)P_3+\tfrac{1}{5}(n+1)(2n+9)P_1,\end{aligned}\right\} \tag{30}$$

which respectively satisfy the following boundary conditions:

$$\left.\begin{aligned}F_n(\pm 1) = 0,\\ G_n(\pm 1) = G_n'(\pm 1) = 0,\end{aligned}\right\} \tag{31}$$

where a prime denotes a derivative. Then, $\tilde{v}$ and $\tilde{w}$ are expanded into series of the polynomials F_n and G_n as follows:

$$\left.\begin{aligned}\tilde{v} &= \sum_{m=0}^{M}\sum_{n=0}^{N} v_{mn}\,G_m(y)\,F_n(z/A),\\ \tilde{w} &= \sum_{m=0}^{M}\sum_{n=0}^{N} w_{mn}\,F_m(y)\,G_n(z/A),\end{aligned}\right\} \tag{32}$$

which automatically satisfy the boundary conditions (29).

On substitution of (32) into (27) and (28) and taking account of the orthogonality of the P_n, we obtain a matrix equation for the unknown expansion coefficients v_{mn} and w_{mn} in the following form:

$$\boldsymbol{A}\boldsymbol{X} = c\boldsymbol{B}\boldsymbol{X}, \tag{33}$$

where

$$\boldsymbol{X} = \begin{pmatrix}\boldsymbol{v}\\ \boldsymbol{w}\end{pmatrix} = (v_{00},\ldots,v_{MN};w_{00},\ldots,w_{MN})^{\mathrm{T}}, \tag{34}$$

represents the unknown vector, $\boldsymbol{A}$ is a matrix whose elements consist of integrals of double or triple products of the P_n and their derivatives and the U_{mn}, and $\boldsymbol{B}$ is a matrix whose elements consist of integrals of double products of the P_n and their derivatives.

The eigenvalue problem of the matrix equation (33) has been solved numerically using the QR algorithm with the double-precision scheme. The eigenvalue of c is thus

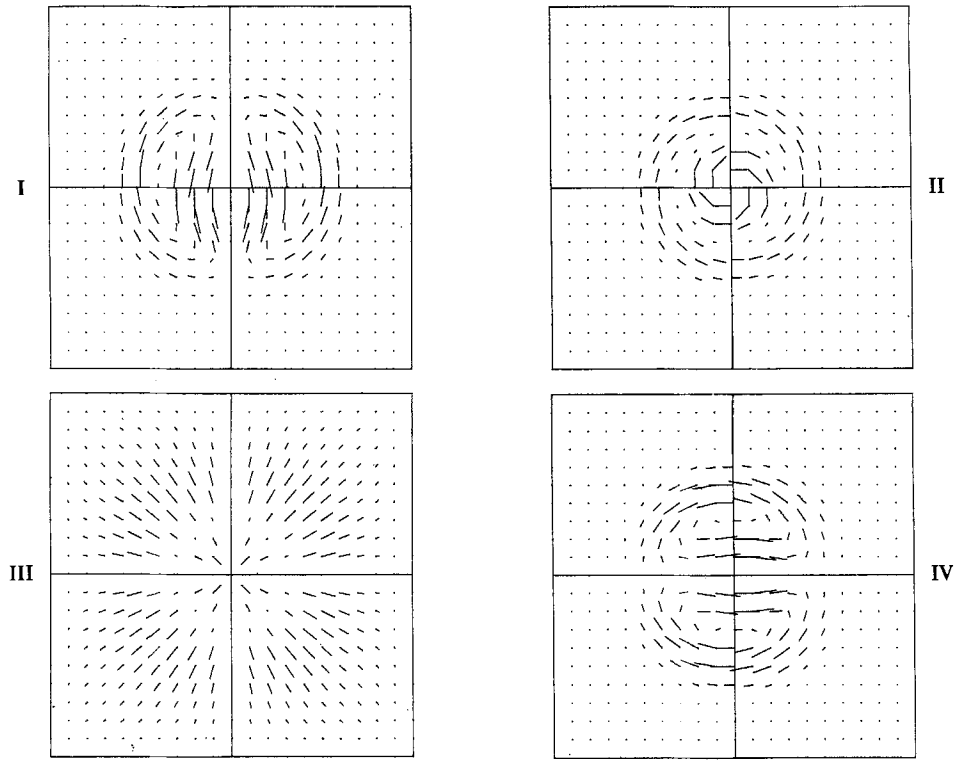

FIGURE 3. Velocity fields of modes I, II, III and IV of the disturbance in the (y, z)-plane. $A = 1$, $R = 1000$, $\alpha = 1.0$, phase arbitrary.

determined for various values of the parameters: the aspect ratio A, the Reynolds number R, and the mode and the wavenumber α of the disturbance. The disturbance velocities $(\tilde{v}, \tilde{w})$ are determined by substituting the numerically obtained eigenvector (34) into (32).

6. Numerical results of the stability

For the basic flow whose velocity $U(y, z)$ is an even function of y and z, as is the case for (12), the disturbance equations allow the following four modes of solution with different parity:

$$\text{I}: (\tilde{v}(\text{e},\text{e}), \tilde{w}(\text{o},\text{o})), \qquad \text{II}: (\tilde{v}(\text{e},\text{o}), \tilde{w}(\text{o},\text{e})),$$

$$\text{III}: (\tilde{v}(\text{o},\text{e}), \tilde{w}(\text{e},\text{o})), \qquad \text{IV}: (\tilde{v}(\text{o},\text{o}), \tilde{w}(\text{e},\text{e})),$$

where, for instance, $\tilde{v}(\text{e},\text{o})$ means that $\tilde{v}$ is an even and odd function of y and z respectively. The general features of the velocity field of each mode may be observed in figure 3 which shows the instantaneous velocity fields of the four modes for $A = 1$, $R = 1000$ and $\alpha = 1$ with unspecified initial phase.

For the square cross-section $A = 1$, the modes I and IV become identical and there remain only three different modes. In the limit of $A \to \infty$, on the other hand, the modes I and II tend to the symmetric $\tilde{v}$-disturbance and the modes III and IV tend to the antisymmetric disturbance, the $\tilde{w}$-component disappearing in either case. The plane Poiseuille flow corresponding to the limit $A \to \infty$ is known to be unstable with

A	3.5	4	5	6	8	∞
R_c	36600	18400	10400	8200	6800	5772
α_c	0.71	0.80	0.91	0.94	0.98	1.02

TABLE 2. Critical values R_c and α_c for the mode-I disturbance

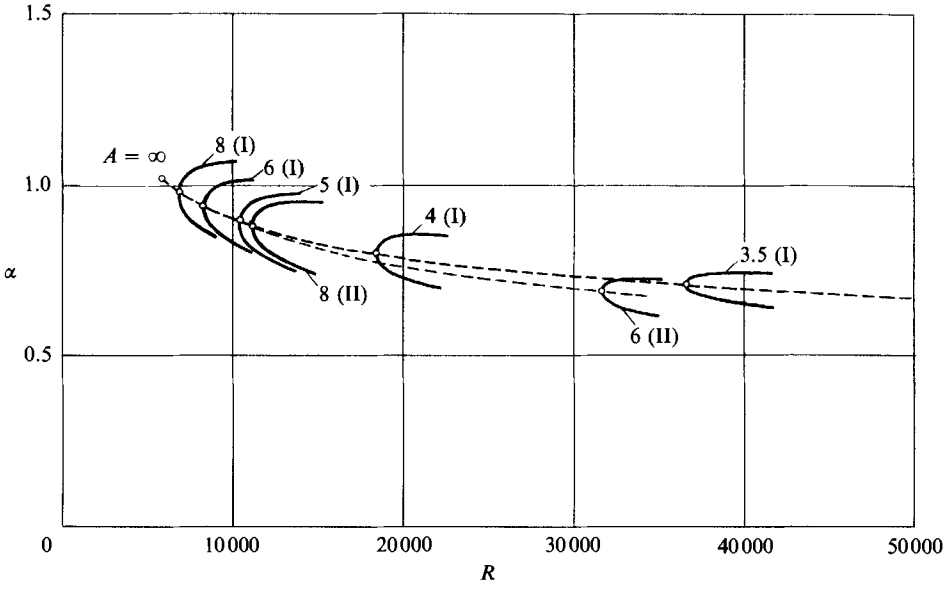

FIGURE 4. Neutral curves near the critical points for various aspect ratios: $A = 8$, 6, 5, 4 and 3.5 for mode I; and $A = 8$ and 6 for mode II.

the critical Reynolds number $R = 5772$ with respect to symmetric $\tilde{v}$-disturbance and stable with respect to the antisymmetric disturbance (Orszag 1971). Thus, modes I and II are expected to have finite critical Reynolds numbers for certain ranges of aspect ratio A, whereas there is no such a guarantee for the modes III and IV.

The stability of the basic flow has been examined with respect to the four modes for Reynolds numbers up to 50000 and wavenumbers below 1.1. It is found that there is no particular mode that is most unstable or least stable throughout all the ranges of the parameters, but mode I is the most unstable in the sense that it becomes unstable first with increasing values of the aspect ratio and the Reynolds number. Thus, according to the eigenvalues of this mode, the flow is stable for small aspect ratios $A \leqslant 3$ and unstable for large ones $A \geqslant 4$ with the critical Reynolds number R_c and the wavenumber α_c as given in table 2.

The value of R_c for each aspect ratio A has been determined as the minimum Reynolds number on the neutral stability curve in the (R, α)-plane as shown in figure 4, and the critical wavenumber α_c is defined as the wavenumber corresponding to $R = R_c$. The values of R_c and α_c for $A = \infty$ have been calculated separately by solving the $\tilde{v}$-disturbance equation in this limit, and they are in perfect agreement with the values given by Orszag (1971) for plane Poiseuille flow, up to the indicated digits.

Figure 4 shows that the critical point (R_c, α_c) for mode I moves along a smooth line with increasing A and seems to approach the point for plane Poiseuille flow in the

A	6	8
R_c	31500	11000
α_c	0.69	0.89

TABLE 3. Critical values R_c and α_c for the mode-II disturbance

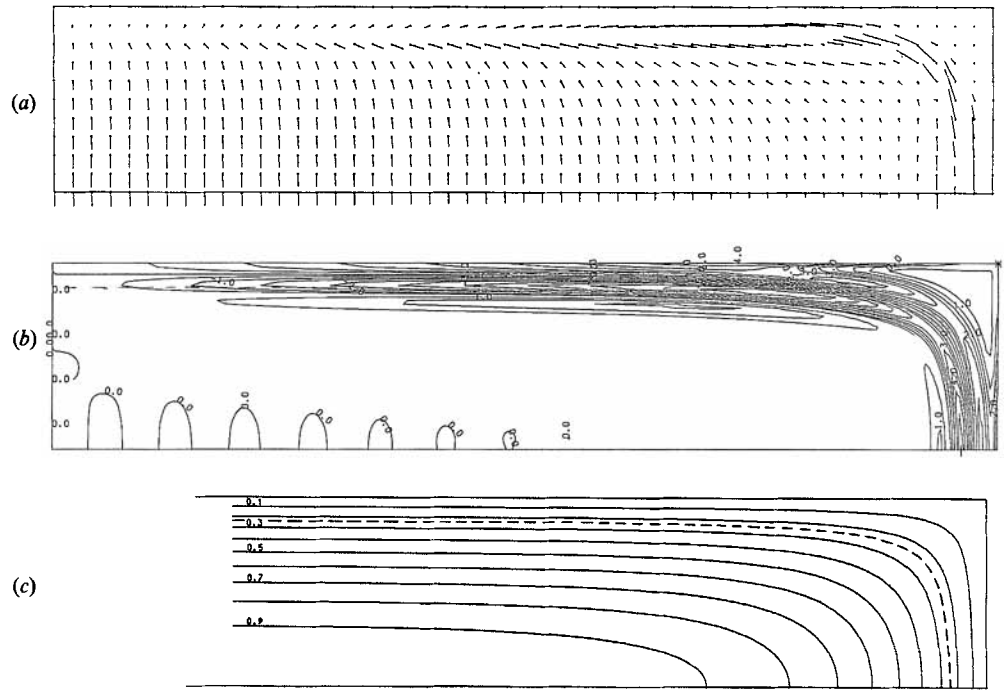

FIGURE 5. Flow patterns of the disturbance in the (y, z)-plane. $A = 5$, $R = 12000$, $\alpha = 0.9$, phase arbitrary. (*a*) Velocity vector field, (*b*) isovorticity contours, (*c*) isovelocity contours of the main flow. Broken line indicates the critical layer, $U = c_r = 0.24$.

limit of $A \to \infty$. With decreasing A, the critical point moves along the line toward larger values of R_c and seems to tend to infinity for a certain critical value of A. It is difficult to determine accurately the critical aspect ratio A_c that separates the stability and instability of rectangular duct flow, but extraporation from the above table gives $A_c = 3.2$ as a rough estimate.

Mode II of the disturbance, which also reduces to the symmetric $\tilde{v}$-disturbance in the limit of $A \to \infty$, is found to be unstable, but with higher value of R_c for each aspect ratio A than mode I, as shown in table 3 and Figure 4.

Modes III and IV, both of which reduce to the stable antisymmetric $\tilde{v}$-disturbance in the limit of $A \to \infty$, are found to be stable for the range of the parameters examined.

The velocity field and the isovorticity contours of the disturbance of mode I in a cross-sectional plane are displayed in figures 5(*a*) and 5(*b*) respectively for $A = 5$, $R = 12000$ and $\alpha = 0.9$. As easily seen from the corresponding neutral curve in figure 4, this disturbance is slightly unstable at $R = 12000$ and stable at $R = 10000$, but the velocity and vorticity fields for these Reynolds numbers are found to be

almost identical to each other. It may be observed in figures 5(*a*) and 5(*b*) that the disturbance fields contain thin regions of very high shear along the critical layer $U = c_r = 0.24$ which is indicated by a broken-line contour in figure 5(*c*).

7. Comparison with experiments

A number of experiments have so far been done on the instability and transition of rectangular duct flows of various aspect ratios. The earlier works by Schiller (1923, $A = 1$ and 3), Davies & White (1928, $A = 38$ to 710), Cornish (1928, $A = 2.92$) and others were, however, all hydraulic experiments which detect the transition by measuring the pressure drop along the flow direction. The critical Reynolds numbers obtained by these authors are considerably lower than theoretical values, but in view of the nature of their measurements it is likely that these experimental values are related with some sort of nonlinear instability rather than the linear instability of present concern.

Direct measurement of the instability of the flow was first made by Kao & Park (1970, $A = 8$) using the modern technique of examining the growth or decay of the controlled artificial disturbances. Their results, expressed as the neutral stability curve in the (R, α)-plane, give the critical Reynolds number $R_c = 2600$ and $\alpha_c = 1.5$. Since their definition of the Reynolds number is based on the hydraulic diameter $d(= 4AL_0/(1+A))$ and the mean velocity $U_m(= Q/4AL_0^2$, Q being the volume flux), their value of R_c for $A = 8$ corresponds to $R_c = 1191$ in the present definition. These experimental values of R_c and α_c do not agree with the corresponding theoretical values for either modes I or II.

At present we have no clear explanation for this discrepancy, but there are some reasons to believe that these experimental values are not related to the linear instability of the flow. First, the flow with a finite aspect ratio A is considered to be stabilized by the presence of the endwalls compared with that of infinite A or plane Poiseuille flow, so that the critical Reynolds number for $A = 8$ should be higher than $R_c = 5772$ for the latter. Theoretical results that give higher critical Reynolds number with decreasing aspect ratio A for both the modes I and II actually support this conjecture. Secondly, the experimental neutral curve covers a much wider wavenumber range than the corresponding theoretical curves in figure 5 and the unstable region includes the zero-wavenumber range which is known to be linearly stable. In view of this the experimental instability obtained by Kao & Park (1970) using controlled excitation could be attributed to a sort of nonlinear subcritical instability. More detailed and precise measurements are needed in order to establish experimentally the linear stability characteristics of the flow.

It is a great pleasure to be able to contribute this article to the special volume of the *Journal of Fluid Mechanics* dedicated to Professor G. K. Batchelor on his seventieth anniversary. This work has been partially supported by the Grant in Aid for Scientific Research from the Ministry of Education, Science and Culture.

REFERENCES

Cornish, R. J. 1928 Flow in a pipe of rectangular cross-section. *Proc. R. Soc. Lond.* A **120**, 691–700.

Davies, S. J. & White, C. M. 1928 An experimental study of the flow of water in pipes of rectangular section. *Proc. R. Soc. Lond.* A **119**, 92–107.

DRAZIN, P. G. & REID, W. H. 1981 *Hydrodynamic Stability*, pp. 216–221. Cambridge University Press.

KAO, T. W. & PARK, C. 1970 Experimental investigations of the stability of channel flows. Part 1. Flow of a single liquid in a rectangular channel. *J. Fluid Mech.* **43**, 145–164.

ORSZAG, S. 1971 Accurate solution of the Orr–Sommerfeld stability equation. *J. Fluid Mech.* **50**, 689–703.

ROSENHEAD, L. (ed.) 1963 *Laminar Boundary Layers*, pp. 492–579. Clarendon.

SAINT-VENANT, B. DE 1855 Mémoire sur la torsion des prismes. *Mémoires de l'Academie des Sciences des Savants Etrangers.* **14**, 233–560.

SCHILLER, L. 1923 Uber den Strömungswiderstand von Rohren verschiedenen Querschnitts und Rauhigkeitsgrades. *Z. Angew. Math. Mech.* **3**, 2–13.

SCHLICHTING, H. 1933 Zur Entstehung der Turbulenz bei der Plattenströmung. *Nachr. Ges. Wiss. Göttingen, Math. – phys. Kl.* 181–208; *Z. Angew. Math. Mech.* **13**, 171–174.

SCHUBAUER, G. B. & SKRAMSTAD, H. K. 1947 Laminar boundary layer oscillations and transition on a flat plate. *J. Res. Natl Bur. Stand.* **38**, 251–292; *J. Aero. Sci.* **14**, 69–78.

TOLLMIEN, W. 1929 Uber die entstehung der Turbulenz. *Nachr. Ges. Wiss. Göttingen*, 21–44.